

Cerenkov radiation in metallic metamaterials

Jin-Kyu So,¹ Jong-Hyo Won,^{1,a)} M. A. Sattarov,¹ Seung-Ho Bak,¹ Kyu-Ha Jang,^{1,b)} Gun-Sik Park,^{1,c)} D. S. Kim,² and F. J. Garcia-Vidal³

¹Department of Physics and Astronomy, Center for THz-Bio Application Systems, Seoul National University, Seoul 151-747, Republic of Korea

²Department of Physics and Astronomy, Center for Subwavelength Optics, Seoul National University, Seoul 151-747, Republic of Korea

³Departamento de Física Teórica de la Materia Condensada, Universidad Autónoma de Madrid, E-28049 Madrid, Spain

(Received 24 June 2010; accepted 3 September 2010; published online 12 October 2010)

The electromagnetic response of a metallic metamaterial to fast-moving electrons is studied by numerical simulations. The considered metamaterial is a one-dimensional array of slits perforated on a metallic film and is found to generate Cerenkov wakes when the electron beam travels near its surface. There is no energy threshold for the generation of such wakes, which would be promising to lower the operation energy of the electron beam in compact Cerenkov free-electron-lasers. Moreover, by analyzing the spectral dependence of the Cerenkov light, it is possible to map the dispersion relation of the guided modes supported by the metamaterial. © 2010 American Institute of Physics. [doi:10.1063/1.3492846]

Cerenkov radiation (CR) applies for electromagnetic (EM) waves that are emitted when a charged particle passes through an insulator at a velocity larger than the speed of light in that dielectric medium.¹ This radiation is usually generated in free-electron-lasers (FELs) and wakefield accelerators²⁻⁶ where choosing the appropriate material is limited by thermal issues⁶ and dielectric breakdown.⁷ In order to overcome these limitations, it would be desirable to find alternative strategies to tune the dielectric properties of the supporting materials. The use of metals for this purpose would be preferable over dielectric materials as they are more robust against the two aforementioned limitations.

In recent years, the concept of EM metamaterials has very much helped in the design of advanced materials whose properties do not exist in Nature.⁸ By placing electric and magnetic resonators in a periodic fashion at a length scale much smaller than the operating wavelength, fascinating EM phenomena such as negative refraction have been experimentally reported.⁹ Along this line, a metamaterial presenting a negative effective refractive index was recently found to support CR emitted in the backward direction.¹⁰

The metamaterial concept has been also applied to plasmonic structures.¹¹ Geometrically induced surface modes with properties mimicking those of surface plasmon polaritons (SPPs) in the optical regime can be built-up by periodically corrugating the surface of a perfect conductor.¹¹⁻¹⁵ Moreover, even a *positive* dielectric response can be achievable from a slab made of a perfect conductor when a one-dimensional (1D) array of slits is drilled into the film.^{12,16-19} It has been shown that in the effective medium limit (wavelength, λ , much larger than the period of the array, d), the dielectric response of the system is dictated by the ratio between d and the width of the slit, a .

In this letter, we show that this metamaterial serves as a tunable dielectric medium which supports threshold-free CR

with the presence of convection electrons. For this purpose, the angles of radiation cones from the real structure and the corresponding effective medium are compared. In the reverse scenario, we also demonstrate how the CR can be used as a tool to measure the dispersion relation of the guided modes supported by the perforated metallic film.

In order to study the interaction between the considered metamaterial and the beam of convection electrons, particle-in-cell (PIC) codes^{20,21} have been used. To identify radiation cones, the dimensions of the structure were assigned as follows: the filling ratio of the slit, $d/a=4$, and the film thickness, $L/d=125/8$. This structure was modeled in the PIC code as a thick film of perfect conductor with cut-through slits as shown in Fig. 1. Then, a Gaussian electron bunch was modeled to pass above the grating with a pulse width of $\sigma/d=1/2$. Two different effective medium theories are currently used to describe the response of a 1D array of slits perforated on a perfect conductor film. The first one maps the structure into an isotropic dielectric medium with an effective refractive index, $\bar{n}=d/a$, and the thickness of the film is also scaled, $\bar{L}=L/\bar{n}$.¹⁶⁻¹⁸ On the other hand, the anisotropic approach, as derived in Refs. 12 and 19, characterizes the system by $\bar{\epsilon}_x=d/a$, $\bar{\epsilon}_z=\infty$, $\bar{\mu}_y=a/d$, $\bar{L}=L$.

In Fig. 2(a) we compare the results of PIC calculation with those from the two effective medium theories. The energy of the electron bunch was varied to verify the well-

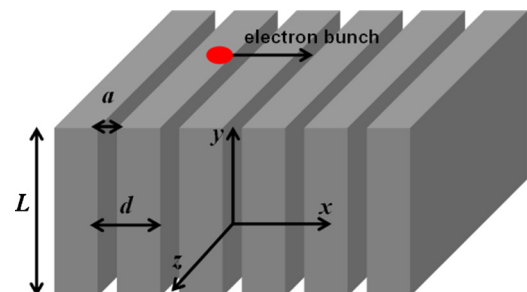


FIG. 1. (Color online) Schematic model of cut-through metal slits with convection electrons.

^{a)}Present address: LIG Nex1, Yongin, Gyeonggi-do, Korea.

^{b)}Present address: Korea Atomic Energy Research Institute, Daejeon, Korea.

^{c)}Electronic mail: gunsik@snu.ac.kr.

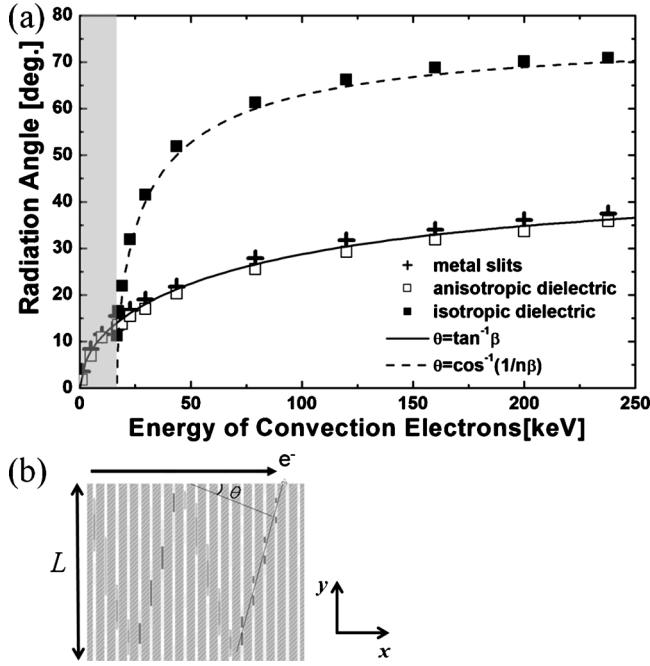


FIG. 2. (a) Simulated radiation angles for metal slits structure and its effective dielectric media are compared at various beam energies. (b) Contour plot of the H_z field distribution for the metamaterial at 20 keV.

known dependence of CR on particle's velocity such as the angle of radiation cone and the velocity threshold found in normal isotropic dielectric medium. Since the energy threshold for an isotropic dielectric medium with $n=4$ is 16.8 keV, the energy of the electron bunch was varied below and above this value. As expected, for the effective isotropic medium with $\bar{n}=d/a=4$, the threshold energy was identified as 16.8 keV below which no radiation is generated as shown in Fig. 2(a).

Figure 2(b) shows the corresponding contour plot for H_z evaluated at 20 keV, where the radiation angle is found to be 14.8° . The electron bunch accompanies EM fields inside slits as it travels down the structure as depicted in this panel, which forms a Cerenkov-like radiation cone. However, its exact dependence on electron's energy does not follow the one for normal isotropic dielectric medium, $\cos\theta=1/n(\omega)\beta$, where θ is the angle formed by the particle velocity \vec{v} and the wave vector of the CR and $n(\omega)$ is the index of refraction at the considered frequency, ω . Rather, since the propagation of radiated field only occurs in the vertical direction inside each slit with the velocity of light, c , while the electron bunch passes above the structure with the velocity of βc , the radiation angles in metal slits follow those from the relation, $\tan\theta=v_{\text{beam}}/c=\beta$, together with those from an effective anisotropic medium as shown in Fig. 2(a). As a result, in contrast to the isotropic dielectric case where velocity threshold is given as $\beta>1/n$, no velocity threshold was found in metal slits and its effective anisotropic dielectric medium. These peculiar characteristics can also be deduced from the well-known kinematic relation for CR in anisotropic dielectric medium, $\cos\theta_0=1/n_j(\omega,\vec{k}/k)\beta$, where $n_j(\omega,\vec{k}/k)$ denotes the refractive index for ordinary- and extraordinary-waves.^{2,3} Since the refractive index at angle θ for extraordinary-waves is given by $\mu/n_e^2(\theta)=\cos^2\theta/\epsilon_o+\sin^2\theta/\epsilon_e$, the kinematic relation becomes $\tan\theta_0=\beta$ for the considered uniaxial crystal with $\epsilon_o=\infty$, $\epsilon_e=d/a$, and μ_x

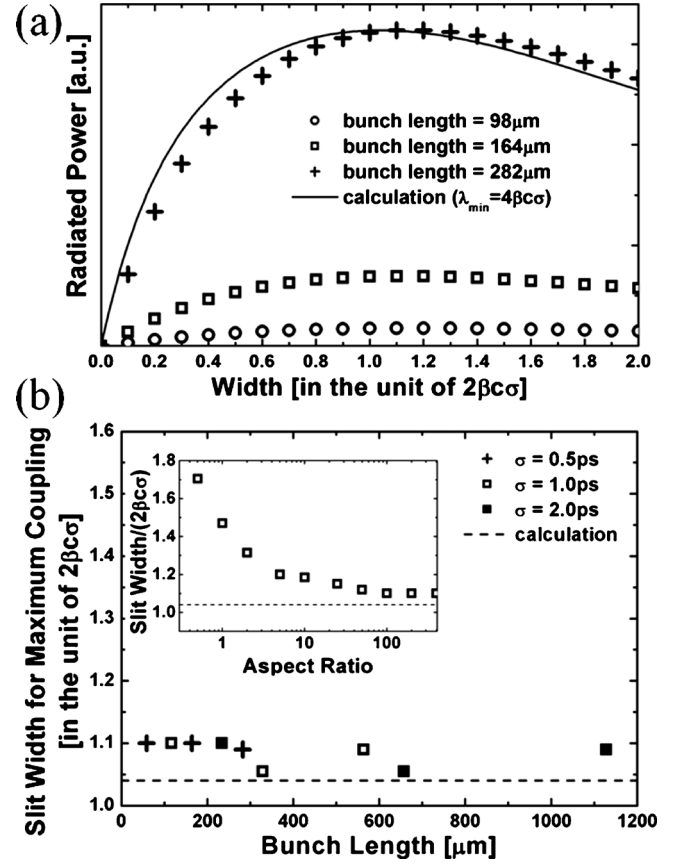


FIG. 3. (a) Coupling efficiencies as a function of slit width for various bunch lengths. (b) The slit widths for maximum coupling are shown for various spatial bunch lengths assuming the aspect ratio of spatial bunch length to thickness of 200 together with those estimated by a simple model (dashed line). The inset shows the effect of the bunch's transverse thickness on the coupling for the fixed spatial bunch length, $2\beta c\sigma=117 \mu\text{m}$.

$=\mu_y=\mu_z=\mu$ with isotropic permeability, μ . However, this approach is not appropriate for the thin film cases where the EM response is better described with the use of guided modes.^{16,17,19} For thin films, discrete guided modes are excited as a result of the phase velocity synchronism with the electron bunch, which will be clarified in the following discussions.

Since the diffraction at each slit opening is the only way through which evanescent waves of the electron bunch can be transformed into propagating waves inside slits, the amount of generated radiation from metamaterials should depend on the profile of slit openings. To examine this dependence, the coupling efficiencies from a convection electron bunch to guided modes of single slit with varying slit widths were simulated and compared with the calculated efficiency based on the method for calculating the SPP-generation efficiency.²² During the comparison, only the relative dependence of coupling efficiency on slit width was examined. For simplicity, the evanescent waves of electron bunch were assumed to have the following spatial dependences:

$$H_z(y) = (N_b)^{-1/2} \exp(i\gamma_b y), \quad (1)$$

where $\gamma_b = \sqrt{\epsilon(\omega/c)^2 - k_b^2}$, $\epsilon = \epsilon' + i\epsilon''$ in metal, and $k_b = \omega/\beta c$. The coupling efficiency, $e(\beta, \sigma)$, of slit mode to an electron bunch with its velocity, βc , and pulse width, σ , is given by

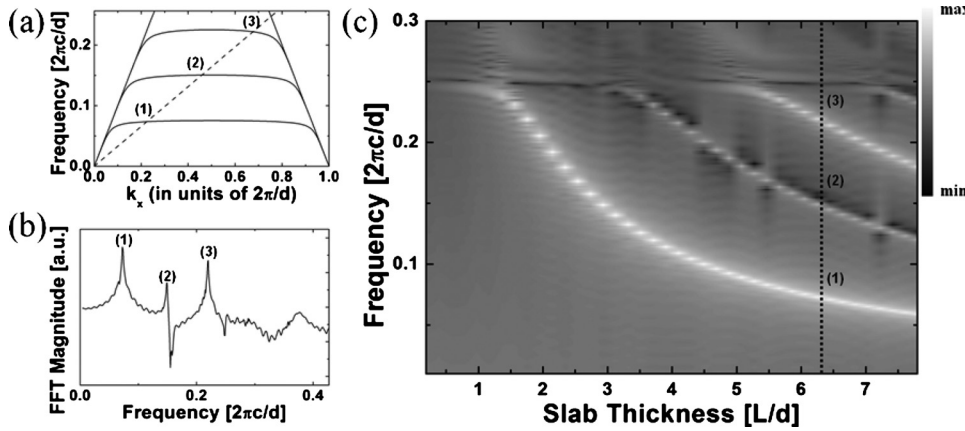


FIG. 4. (a) Dispersion of the first three guided modes for metal slits having $d/a=4$ and $L/d=25/4$ with 30 keV beam line (dashed line) and (b) The fast Fourier transform (FFT) spectrum of H_z field measured in the middle of the center slit. (c) FFT spectrum for H_z as a function of slab thickness.

$$e(\beta, \sigma) = (N_e)^{-1/2} \int_0^\infty |\alpha(w, \omega)|^2 \exp[-(\beta\sigma)^2 \omega^2 / 2] d\omega, \quad (2)$$

where w is the slit width, N_e is the normalization constant, $\alpha = \alpha(w/2) = (1/i) \{ (4/\pi) [(\beta^2 - 1)^{-1/2} - (\beta^2 - 1)^{-1} - i\epsilon'' - 1] (w/2\pi c/\omega) \}^{1/2} [I_1/1 + (w/2\pi c/\omega)I_0]$, $u^2 + (\gamma_u)^2 = 1$, $I_0 = \int_{-\infty}^\infty du [\sin c^2(wu/2c/\omega)/\gamma_u]$, and $I_1 = \int_{-\infty}^\infty du (\sin c^2(wu/2c/\omega) \cos(wu/2c/\omega)/\gamma_u \{ \gamma_u + [(\beta^2 - 1)^{-1} - i\epsilon'' + 1]^{-1/2} \})$. By reciprocity, this coefficient also gives the scattering coefficient from evanescent waves of the electron bunch to slit mode. Therefore, we can predict how efficiently the radiation will be generated according to various slit widths.

To verify this, the radiated power inside the single slit was recorded for a Gaussian electron bunch with various energies and temporal durations. As shown in Fig. 3(a), the calculated coupling efficiency agrees closely with the simulated efficiencies showing maxima at $w \approx 1.04/(2\beta c\sigma)$, which confirms that the radiation in metal slits originates from the diffraction at each slit opening. Moreover, the slit width for maximum coupling is almost remained constant regardless of the spatial bunch length, $2\beta c\sigma$, as shown in Fig. 3(b). As the bunch becomes thinner, it approaches the calculated value as shown in the inset of Fig. 3(b), which is assuming 10 keV–1 ps electron bunch.

CR has been employed to diagnose the photonic information of such structures as photonic crystals,²³ plasmonic crystals,²⁴ and perfect invisibility cloaking metamaterials.²⁵ In the same manner, the predicted guided modes¹⁶ of the present metamaterial can also be probed. In Fig. 4(a), the phase velocity of the bunch matches with that of the guided modes at the normalized frequencies of 0.073, 0.149, and 0.222. Due to this synchronism, the frequency spectrum of the excited H_z field shows resonant peaks at 0.073, 0.149, and 0.218 as shown in Fig. 4(b), which confirms the existence of geometrically induced guided modes.

To corroborate the existence of guided modes, the film thickness, L/d , was varied from 0.2 to 7.8 and the corresponding spectrum of H_z field is plotted in Fig. 4(c). As the thickness increases, more resonantly excited states appear due to the introduction of higher order modes. Furthermore, the absence of resonances above the frequency of 0.248 is due to the onset of Smith–Purcell radiation.

In conclusion, we have shown that a metallic metamaterial supports energy threshold-free Cerenkov-like wakes when a bunch of electrons moves close to it. The detailed energy dependence of the angles of such wakes confirms the

effective behavior of the structure as an anisotropic dielectric medium. The predicted guided modes have been also identified from the spectrum of resonantly excited states. The robustness of the threshold-free metamaterial to dielectric breakdown and thermal issues would be promising for applications such as Cerenkov FELs and wakefield accelerators.

This work was supported by National Research Foundation of Korea Grant funded by the Korean Government (Grant No. 2009-0083512).

¹P. A. Cherenkov, Dokl. Akad. Nauk SSSR 2, 451 (1934).

²V. L. Ginzburg, Sov. Phys. Usp. 2, 874 (1960).

³J. V. Jelley, *Cerenkov Radiation and Its Applications* (Pergamon, London, 1958).

⁴G. T. di Francia, Nuovo Cim. 16, 61 (1960).

⁵E. E. Fisch and J. E. Walsh, Appl. Phys. Lett. 60, 1298 (1992).

⁶T. J. Owens and J. H. Brownell, J. Appl. Phys. 97, 104915 (2005).

⁷M. C. Thompson, H. Badakov, A. M. Cook, J. B. Rosenzweig, R. Tikhoplav, G. Travish, I. Blumenfeld, M. J. Hogan, R. Ischebeck, N. Kirby, R. Siemann, D. Walz, P. Muggli, A. Scott, and R. B. Yoder, Phys. Rev. Lett. 100, 214801 (2008).

⁸J. B. Pendry, A. J. Holden, W. J. Stewart, and I. Youngs, Phys. Rev. Lett. 76, 4773 (1996); J. B. Pendry, A. J. Holden, D. J. Robbins, and W. J. Stewart, IEEE Trans. Microw. Theory Tech. 47, 2075 (1999); for a recent review see V. M. Shalaev, Nat. Photonics 1, 41 (2007).

⁹R. A. Shelby, D. R. Smith, and S. Schultz, Science 292, 77 (2001).

¹⁰S. Xi, H. Chen, T. Jiang, L. Ran, J. Huangfu, B. I. Wu, J. A. Kong, and M. Chen, Phys. Rev. Lett. 103, 194801 (2009).

¹¹J. B. Pendry, L. Martín-Moreno, and F. J. García-Vidal, Science 305, 847 (2004).

¹²F. J. García-Vidal, L. Martín-Moreno, and J. B. Pendry, J. Opt. A, Pure Appl. Opt. 7, S97 (2005).

¹³A. P. Hibbins, B. R. Evans, and J. R. Sambles, Science 308, 670 (2005).

¹⁴F. J. García de Abajo and J. J. Sáenz, Phys. Rev. Lett. 95, 233901 (2005).

¹⁵A. P. Hibbins, M. J. Lockyear, I. R. Hooper, and J. R. Sambles, Phys. Rev. Lett. 96, 073904 (2006).

¹⁶J. T. Shen, P. B. Catrysse, and S. Fan, Phys. Rev. Lett. 94, 197401 (2005).

¹⁷P. B. Catrysse, G. Veronis, H. Shin, J. T. Shen, and S. Fan, Appl. Phys. Lett. 88, 031101 (2006).

¹⁸A. Pimenov and A. Loidl, Phys. Rev. B 74, 193102 (2006).

¹⁹J. Shin, J. T. Shen, P. B. Catrysse, and S. Fan, IEEE J. Sel. Top. Quantum Electron. 12, 1116 (2006).

²⁰B. Goplen, L. Ludeking, D. Smithe, and G. Warren, Comput. Phys. Commun. 87, 54 (1995).

²¹CST Studio Suite, 2008, <http://www.cst.com>.

²²P. Lalanne, J. P. Hugonin, and J. C. Rodier, Phys. Rev. Lett. 95, 263902 (2005).

²³F. J. García de Abajo, A. G. Pattantyus-Abraham, N. Zabala, A. Rivacoba, M. O. Wolf, and P. M. Echenique, Phys. Rev. Lett. 91, 143902 (2003).

²⁴Y. M. Shin, J. K. So, K. H. Jang, J. H. Won, A. Srivastava, and G.-S. Park, Phys. Rev. Lett. 99, 147402 (2007).

²⁵B. Zhang and B. Wu, Phys. Rev. Lett. 103, 243901 (2009).